Supporting Information

In-Situ Self-Assembled Near-Infrared Phototherapeutic Agent: Unleashing Hydrogen Free Radicals and Coupling with NADPH Oxidation

Yingcui Bu[a,b], Zhi-Peng Yu[a], Zhou Lu[d], Haoran Wang[e], Yu Deng [a], Xiaojiao Zhu[*a], and Hongping Zhou[*a,c]

[a]School of Chemistry and Chemical Engineering, Institute of Physical Science and Information Technology, Anhui University, Key Laboratory of Functional Inorganic Materials Chemistry of Anhui Province, Key Laboratory of Chemistry for Inorganic/Organic Hybrid Functionalized Materials of Anhui Province, Key Laboratory of Structure and Functional Regulation of Hybrid Materials (Anhui University) Ministry of Education, Hefei, 230601, P.R. China

[b]School of Materials and Chemistry, Anhui Agricultural University, 230036, Hefei, P.R. China

[c]School of Chemical and Environmental Engineering, Anhui Polytechnic University, 241000, Wuhu, P.R. China

[d]School of Physics and Electronic Information, Anhui Normal University, Wuhu 241002, China

[e]School of Chemistry and Chemical Engineering, Nanjing University of Science and Technology, 210094, Nanjing, P.R. China

*Corresponding author.

Email: zhpzhp@263.net (Hongping Zhou); xiaojzhu@ahu.edu.cn (Xiaojiao Zhu)

Table of Contents

Experimental Procedures

Main Materials. 2, 7-dichloro fluorescein diacetate (DCFH-DA), 9,10-anthracenediylbis (methylene) dimalonic acid (ABDA), 5,5-Dimethyl-1-pyrroline N-oxide (DMPO), 2, 2, 6, 6-tetramethylpiperidinyl-1-oxide (TEMPO), 4-Vinylbenzoic acid (PVBA) Mito Tracker™ Deep Red FM, DAPI, 3-(4, 5-dimethylthiazol-2-yl)-2, 5-diphenyltetrazolium bromide (MTT), Singlet Oxygen Sensor Green (SOSG), Mitochondrial membrane potential assay kit with JC-1, Calcein-AM/propidium iodide (PI) live/dead cells kit, CellTitler-Glo® Cell Viability kit, ROS-ID® Hypoxia/Oxidative stress detection kit, BODIPY™ 581/591 C11, reduced coenzyme (NADPH), Cyanine 3 (Cy3), erastin, ferrostatin-1 (Fer-1) and so on, were obtained from commercial sources (Aladdin, Macklin, Sigma-Aldrich, Bioquest, Thermo and Promega). Human hepatocellular carcinoma cell (HepG2), Human cervical cancer cell (HeLa cells) and A549 cell were purchased from BeNa culture collection, ICR (Institute of Cancer Research) female mice were provided by Anhui Qingyuan Animal Co., Ltd. All commonly chemical reagents were analyzed pure grade and used without further purification.

Instruments. Nuclear magnetic resonance (NMR) spectra were measured on a (400 MHz Bruker AVANCE instruments using the dimethyl sulfoxide-d6 (DMSO-d_6) as solvents. Mass spectra were performed on a mass spectrometer with LTQ Orbitrap XL. Absorption spectra were measured using UV-265 spectrophotometer. Fluorescence spectra were recorded on a Hitachi F-4500 fluorescence spectrophotometer. EPR spectrum was recorded on a Bruker Nano x-band spectrometer. High resolution transmission electron microscopy (HRTEM) of as-prepared nanoparticles were performed by a JEM-2100F and JEM-F200 field emission transmission electron microscope. The atomic force microscopy (AFM) and surface potential were recorded on the the Atomic Force Microscope with Kelvin Probe (AFM 5500M). The electrochemical measurements were conducted on an electrochemical workstation (Chenhua CHI-660E) in a standard three-electrode cell, *in vitro* and cell imaging was showed on TCS SP8 DIVE/SP8 DIVE confocal laser scanning microscope (CLSM) with 10 × or 60 × objective lens.

Synthesis and Characterization

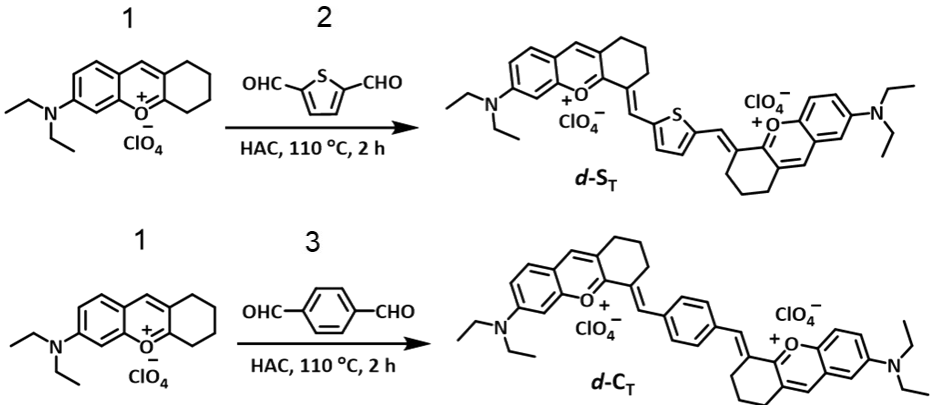

Scheme S1 General synthetic procedure for the preparation of ***d*-S$_T$** and ***d*-C$_T$**.

Synthesis of *d*-S$_T$. Compound **1** [s1] (2.79 g, 7.85 mmol) and Compound **2** (0.5 g, 3.57 mmol) were dissolved in acetic acid (20 mL), and the reaction mixture was heated to 110° for 2 h. After finished, the solvent was removed under reduced pressure to give the crude product, which was purified by silica gel flash chromatography using CH_2Cl_2/ethanol (10:1) as eluant to get black solid ***d*-S$_T$** (yield 45 %). ^{1}HNMR (400 MHz, DMSO-d_6), δ (ppm): 8.41 (s, 2 H), 8.27 (s, 2 H), 7.82-7.79 (t, J = 6.9 Hz, 4 H), 7.44-7.41(d, J = 8.48 Hz, 2 H), 7.21(s, 2 H), 3.71-3.69(d, J = 6.44 Hz, 8 H), 2.93-2.86 (d, J = 28 Hz, 8 H), 1.97-1.94 (t, J = 2.64 Hz, 4 H), 1.27-1.23 (t, J = 6.66 Hz, 12 H).^{13}C NMR (100 MHz, DMSO-d_6), δ (ppm): 161.57, 158.87, 156.48, 145.26, 141.22, 132.59, 124.89, 119.86, 109.87, 95.91, 87.49, 46.26, 27.67, 27.20, 21.13.MS (ESI): calcd for: $C_{40}H_{44}N_2O_2S^{2+}$ $[M/2]^{2+}$, 308.1557; found,308.1566.

Synthesis of *d*-C$_T$. Compound **1** (2.92 g, 8.2 mmol) and Compound **3** (0.5 g, 3.72 mmol) were dissolved in acetic acid (15 mL), and the reaction mixture was heated to 110° for 2 h. After finished, the solvent was removed under reduced pressure to give the crude product, which was purified by silica gel flash chromatography using CH_2Cl_2/ethanol (10:1) as eluant to get black solid ***d*-C$_T$** (yield 63 %). ^{1}H NMR (400 MHz, DMSO-d_6), δ (ppm): 8.54 (s, 2 H), 8.07-8.06 (t, J = 1.66 Hz, 2 H), 7.92-7.89 (m, 2 H), 7.77-7.76 (t, J = 1.9 Hz, 4 H), 7.51-7.48 (m, 2 H), 7.29-7.28 (d, J = 1.72 Hz, 2 H), 3.71 (s, 8 H), 2.98-2.88 (d, J = 40 Hz, 8 H), 1.86 (s, 4 H), 1.24 (s, 12 H).^{13}C NMR (100 MHz, DMSO-d_6), δ (ppm):161.63, 159.21, 156.75, 149.22, 134.75,

132.73, 131.52, 130.28, 124.35, 120.23, 119.53, 95.96, 46.29, 27.30, 21.70. MS (ESI): calcd for: $C_{42}H_{46}N_2O_2^{2+}$ $[M/2]^{2+}$, 305.1774; found, 305.1805.

DFT Calculation. Ground state structures of monomers or dimers of ***d*-C_T** and ***d*-S_T** were optimized by DFT with B3LYP functional and 6-31G basis set. The excited state related calculations (UV-vis absorption) were carried out with the time dependent DFT (TD-DFT) with the optimized structure of the ground state (DFT/6-31G).

Procedure of Transmission Electron microscope (TEM). ***d*-C_T** and ***d*-S_T** (10 μM) assembled in deionized water at different time points (10 min, 20 min, 30 min). Subsequently, the morphology of the as-prepared nano assemblies were observed using JEM-2100F and JEM-F200 transmission electron microscope.

Procedure of Atomic Force Microscope (AFM). ***d*-C_T** and ***d*-S_T** (10 μM) assembled in deionized water for 30 min. Subsequently, the morphology of the as-prepared nano assemblies were analyzed using SPM-8100FM atomic force microscope.

Photocatalytic NADPH Oxidation. Photocatalysis between the as-prepared compounds (10 μM) and NADPH ($A_{340\ nm}$= 1) in H_2O (DMSO/H_2O= 1:100, v/v, pH= 7.4) without or with light irradiation under air or N_2 atmosphere for different time (0 ~ 90 s) were assessed by UV-Vis spectroscopy at 298 K [S2].

Singlet Oxygen Generation. 9, 10-anthracenediyl bis(methylene) dimalonic acid (ABDA) was obtained to detect the production of singlet oxygen ($^1O_2$). In detail, ***d*-C_T** or ***d*-S_T** (10 μM) in H_2O was mixed with ABDA (100 μM) under air or N_2 atmosphere. Then the absorbance of ABDA in dark or irradiation (660 nm laser; 200 mW) for 0 ~ 100 s, respectively was monitored by UV-vis at 298 K.

H• Detection by Electron Paramagnetic Resonance (EPR) Assay. Compounds were dissolved in H_2O at a dilution of 10 μM, and then 500 mM DMPO was added into the test solution, without and with irradiation (660 nm laser; 200 mW) for 1 min. Finally, The EPR assay was carried out with a Bruker Nano x-band spectrometer at room temperature.

Photoelectrochemical Tests. Firstly, the powder (5 mg) of ***d*-$\mathbf{C_T}$** or ***d*-$\mathbf{S_T}$** was dispersed in 0.5 mL mixed solution of Nafion and ethanol (1 mL Nafion (5 wt %) and 9 mL ethanol) and sonicated for 30 min to obtain a slurry. Then, the slurry (100 uL) was drop-coated onto the ITO glass (coating area: 1 cm × 1 cm). After the materials were dried on the glass, the experiment was started. During the tests, the bias voltage of 0.5 V was added on the electrode. LED light was used to irradiated on the ITO gap, and the electrochemical measurements, including transient photocurrent responses, electrochemical impedance spectra and cyclic voltammetry (CV) curve were conducted on an electrochemical workstation (Chenhua CHI-660E) in a standard three-electrode cell, in which the Ag/AgCl (containing saturated KCl solution), platinum (Pt) foil, and compound scoated ITO were used as the reference electrode, counter electrode, and working electrode, respectively. The Na_2SO_4 aqueous solution (0.1 M) was used as the electrolyte [S3].

Cell Culture. Different cells lines were cultured in cell culture dishes with Dulbecco's modified eagle medium (DMEM) medium containing 10 % fetal bovine serum (FBS) and incubated in air atmosphere (37°, 5 % CO_2). For fluorescence imaging, the cells were planted into glass bottom dishes (15 × 15 mm) at density of $10^4 \sim 10^6$. Before imaging, the dishes were washed with PBS (pH 7.2) for three times.

For hypoxia treatment, after being planted into glass bottom dishes (15 × 15 mm) at a density of $10^4 \sim 10^8$, the cell dishes were transferred to a hypoxia chamber (2 % O_2, 5 % CO_2, and 93 % N_2) and incubated for another 8 h at 37°. Notably, to ensure cellular hypoxia to the utmost extent, after hypoxia incubation for 8 h, cell medium involved in the incubation of compounds (10 μM) or commercial materials should be bubbled for 10 minutes in advance with a mixed gas (5 % CO_2, and 95 % N_2) [S4].

Cell uptake Assay. HepG2 cells were seeded into confocal dishes and incubated for 48 h. After incubated with 10 μM of compounds for 10 min and 30 min,respectively (37°, 5 % CO_2) , fluorescence images were promptly captured by the CLSM.

Subcellular Colocalization Assay. HepG2 cells were seeded into confocal dishes and incubated for 48 h. After incubated with 10 μM of compounds for 30 min (37°, 5 %

CO_2), the cells were further stained by 1μM Mito Tracker™ Deep Red FM (λ_{ex} = 640 nm; λ_{em} = 659 nm) and 1μM DAPI (λ_{ex} = 405 nm; λ_{em} = 420 ~ 450 nm). Fluorescence images were promptly captured by the CLSM.

Detection of $^1O_2$ in living cells. SOSG was used for the intracellular $^1O_2$ probe. Firstly, cells were incubated with compounds (10 μM) for 30 min followed by incubation with 2 μM SOSG (λ_{ex}= 504 nm; λ_{em}= 525 nm) for another 15 min. And then the green fluorescence signals were immediately observed by CLSM.

Detection of $O_2^{-\bullet}$ in living cells. Dihydroethidium (DHE) was used as an $O_2^{-\bullet}$ indicator to detect intracellular $O_2^{-\bullet}$generation. HepG2 cells were planted onto 15-mm confocal dishes with incubation for 24 h under hypoxic (2 % O_2) conditions, Afterwards, 10 μM of ***d*-S_T** was added and incubated for another 30 min followed by incubation with 2 μM DHE (λ_{ex}= 560 nm; λ_{em}= 650 nm). for 0.5 h. After irradiation with a 660 nm laser (200 mW) for 100 s, fluorescence images were promptly captured by the CLSM.

Intracellular ATP Detection. After being cultured in 96-well plates for 24 h (37°, 5 % CO_2), the cells were exposed to different concentrations of ***d*-S_T** for 6 h. Then, cells were exposed to 660 nm laser irradiation for 90 s and allowed to recover for another 4 h. Subsequently, CellTiter-Glo reagent was added to each well, and the plate was shaken for 2 min. After incubation at room temperature for 10 min to stabilize the luminescent signal, luminescence intensity was recorded using a microplate reader.

Live/Dead Cell Co-Staining. Standard Calcein-AM/PI Double Stain Kit was used for live/dead cells co-staining assay, where Calcein-AM for live cells (green) and PI for dead cells (red). Briefly, cells were planted onto dishes (15 mm × 15 mm) for adhesion 48 h. Then the cells were treated with 400 uL of dye diluent, 10 uL of Calcein-AM and 5 uL of PI after compounds (10 μM) was added for 30 min. (Calcein-AM: λ_{ex}= 490 nm; λ_{ex} = 520 nm, PI: λ_{ex}= 561 nm; λ_{ex} = 650 nm).

Statistical Analysis. Data were presented as mean ± standard deviation (s.d.) derived from n ≥ 3 independent biological replicates. Graphs and statistical analyses were conducted using GraphPad Prism v8. Statistical significance was assessed using an

unpaired two tailed Student's *t*-test and 95 % confidence intervals for categorical variables. And the P values are indicated in the plot. For all tests, *N.S.* meant no significant difference.

Antitumor Therapy. 10^8 cells/mL of H22 cell suspension was prepared and then subcutaneously injected at the ICR female mice (4 ~ 5 weeks old). After 7-days' inoculation, the tumor size was appropriate and the tumor mice were split into four groups (3 mice each), treated as below: (a) Control, (b) Laser, (c) ***d*-S_T** alone (10^{-5} M, 200 μL), (d) Laser + ***d*-S_T**. During *in vivo* treatment process, the changes of tumor volume and relative body weight were measured every 3 days [S5] . The *in vivo* study was conducted in accordance with the Animal Care and Institutional Ethical Guidance in China. The experiment was authorized by the Animal Research Ethics Committee of Anhui University (certicate number: IACUC(AHU)-2023-007).

***In Vivo* Biosafety Assay.** After 18 days of treatment, all mice were sacrificed, and all normal organs (heart, liver, spleen, lung, and kidney) and tumor tissue were collected for histological analysis via H&E staining.

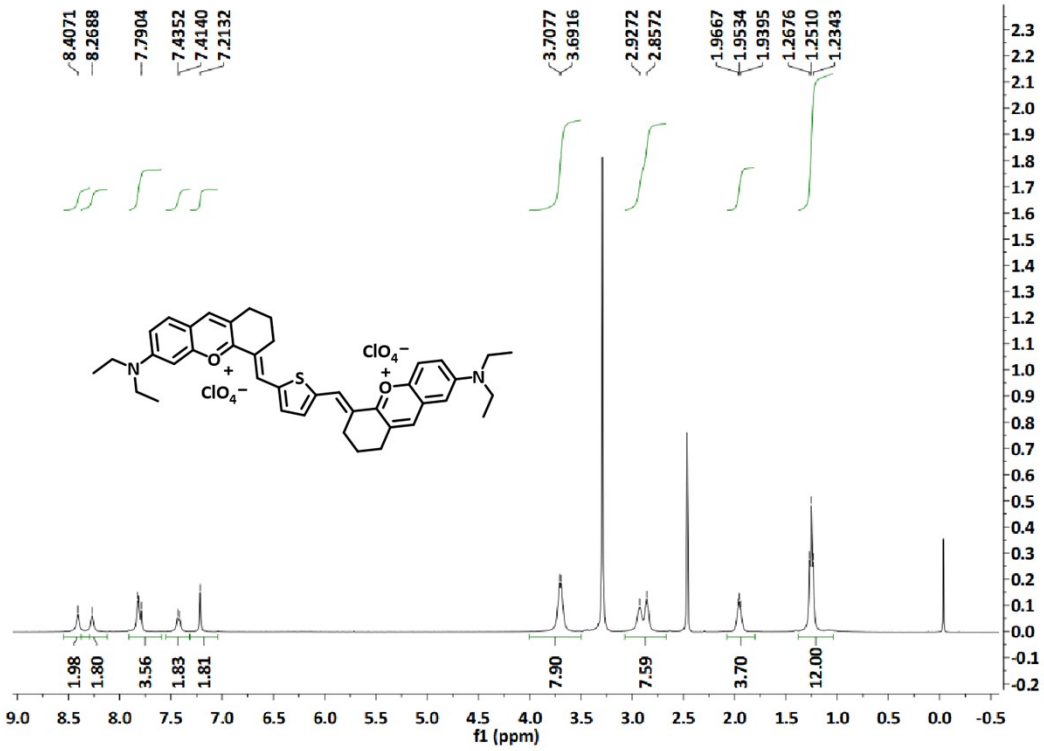

Figure S1 ^{1}H NMR spectrum of ***d*-S$_T$** in DMSO at room temperature.

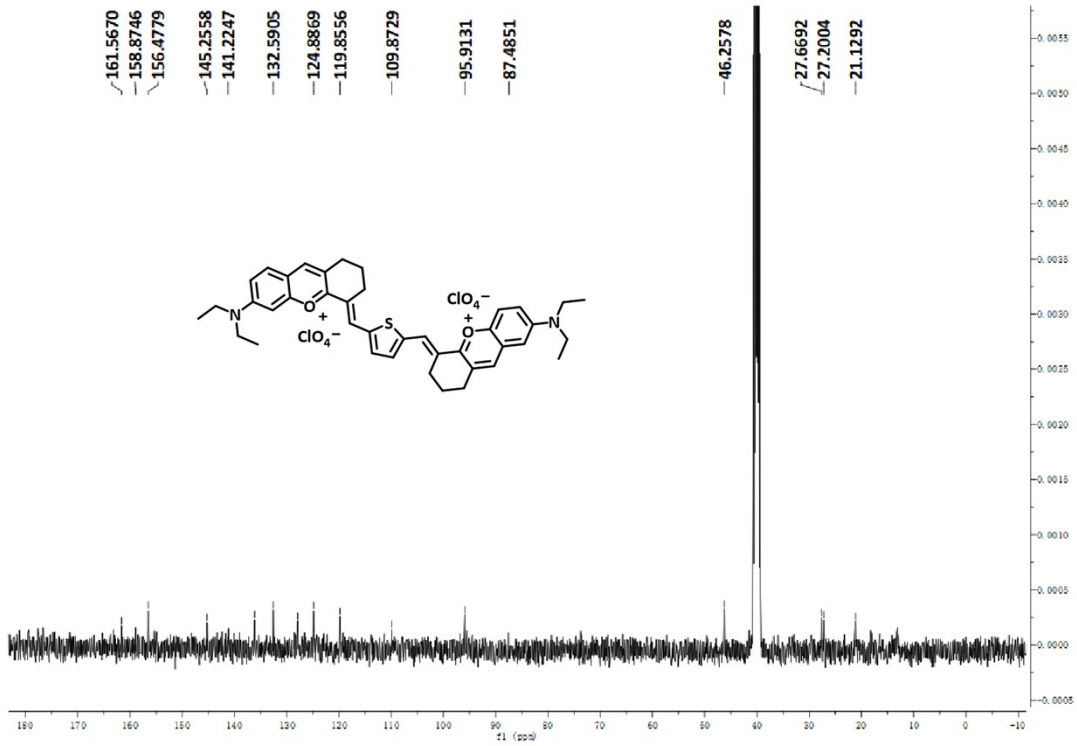

Figure S2 ^{13}C NMR spectrum of ***d*-S$_T$** in DMSO at room temperature.

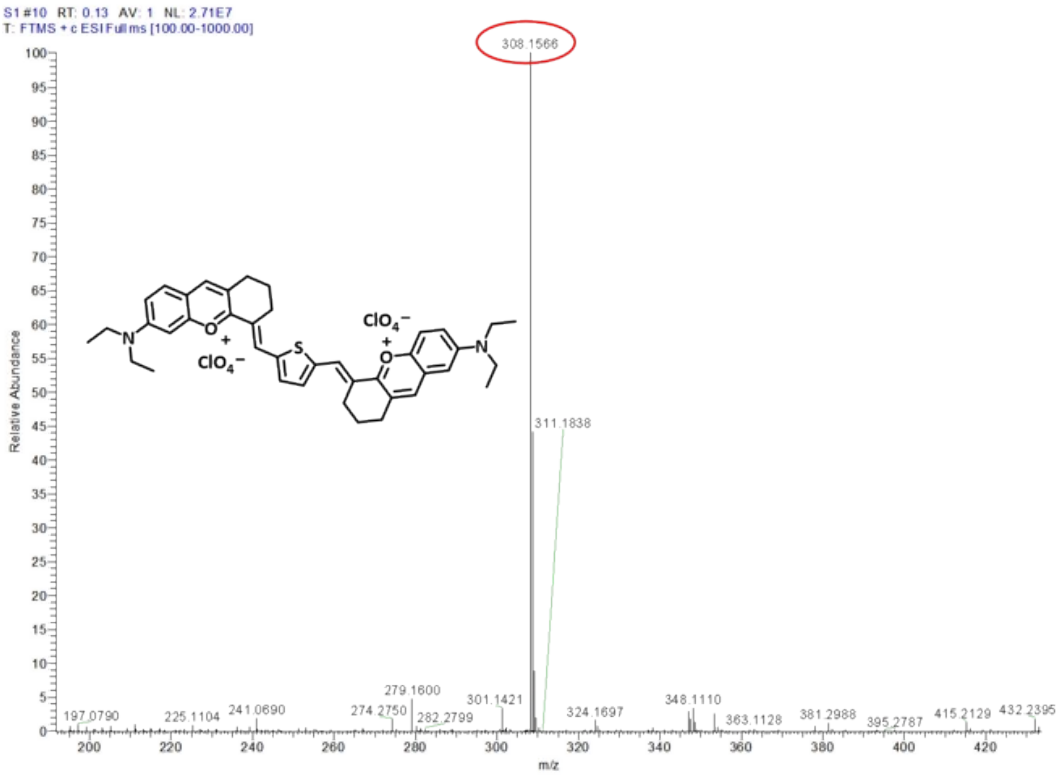

Figure S3 ^{1}H NMR spectrum of ***d*-S$_T$** in DMSO at room temperature.

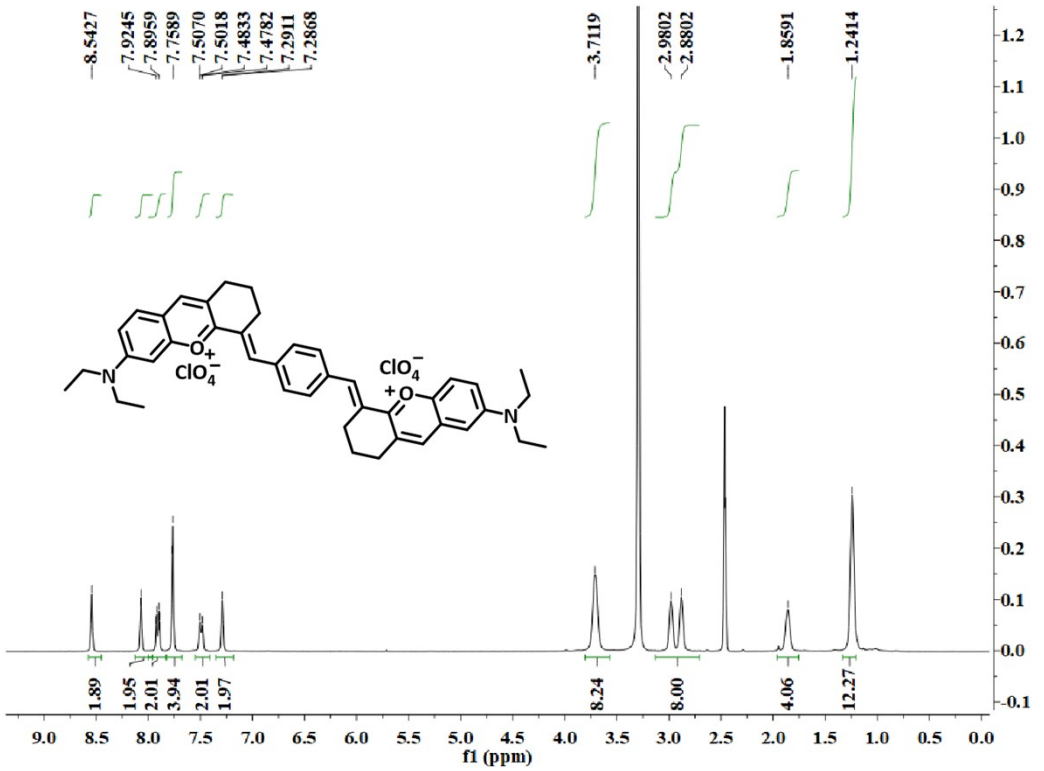

Figure S4 ^{1}H NMR spectrum of ***d*-C_T** in DMSO at room temperature.

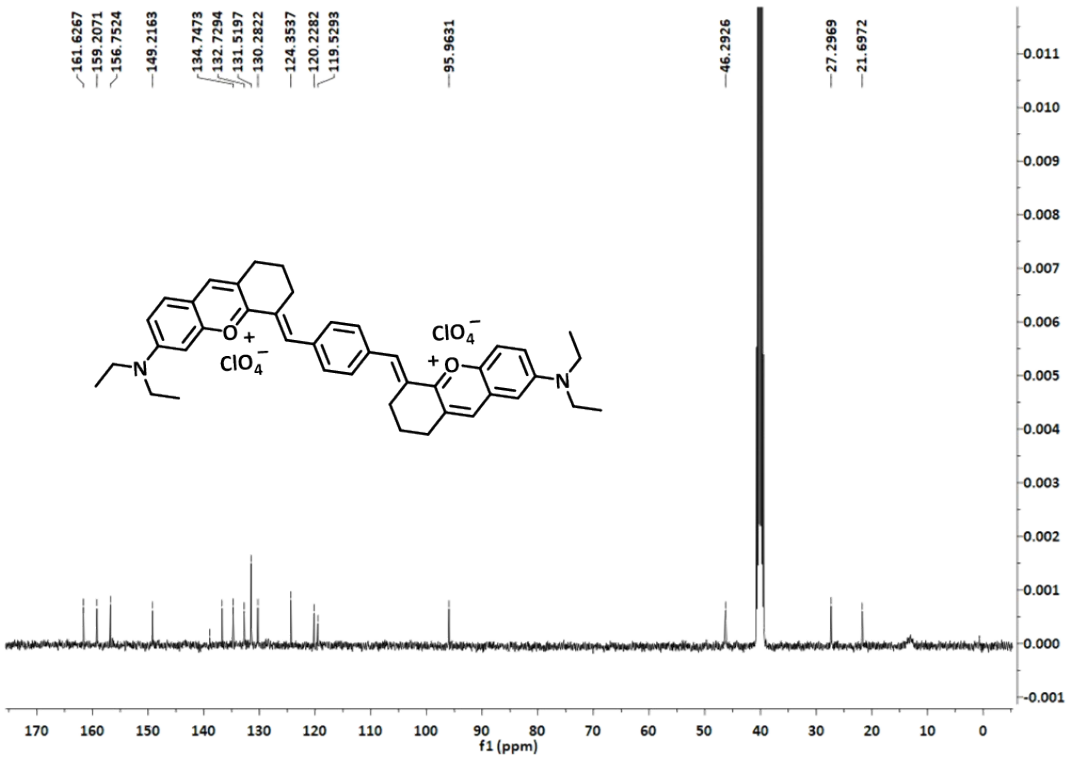

Figure S5 ^{13}C NMR spectrum of ***d*-C_T** in DMSO at room temperature.

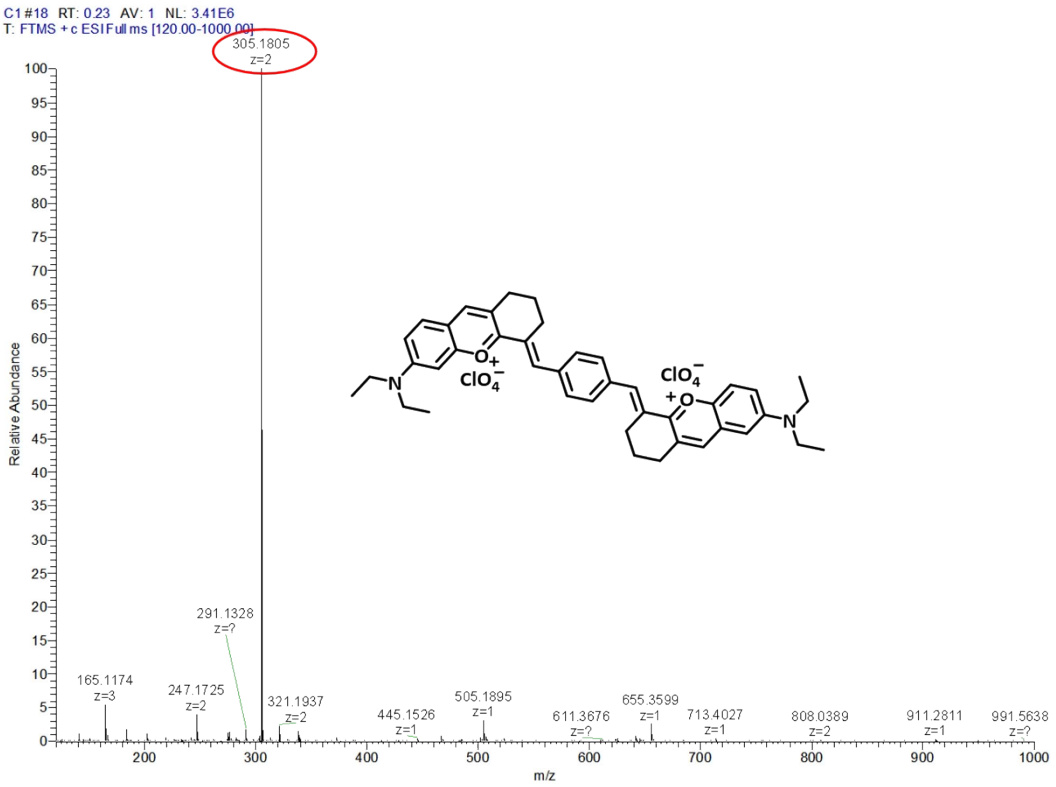

Figure S6 HRMS spectrum of ***d*-C_T**.

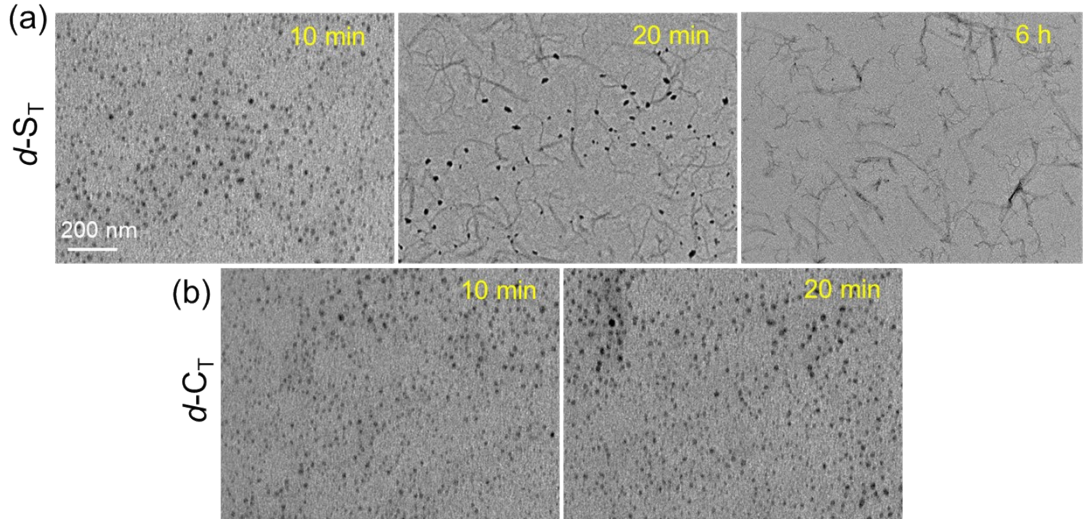

Figure S7 TEM images of assembled ***d*-S_T** (a) and ***d*-C_T** (b) in deionized water at different time points.

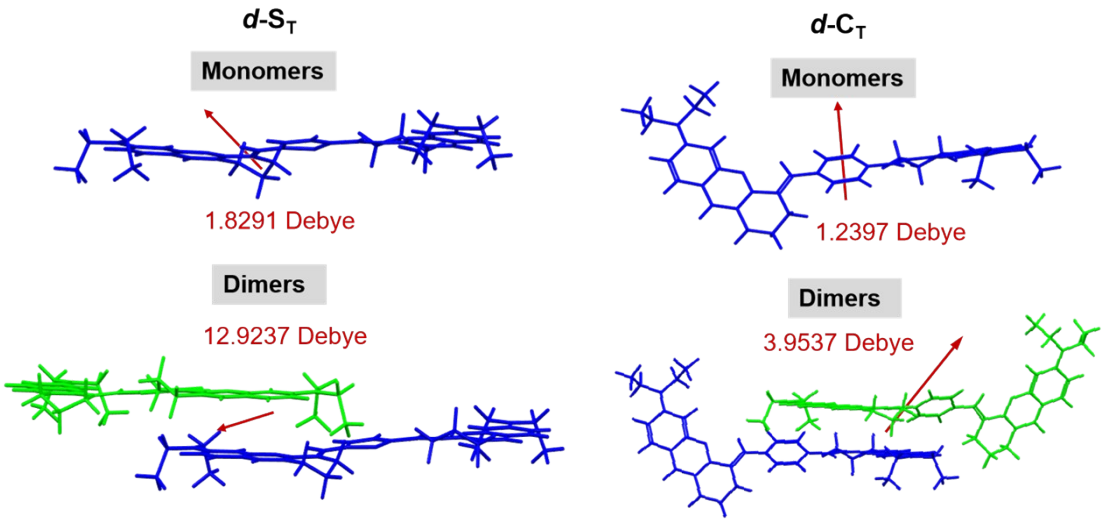

Figure S8 The molecular structures and dipole moment of monomer and dimers calculated using density functional theory (DFT) method at the B3LYP/6-31G (d, p) level.

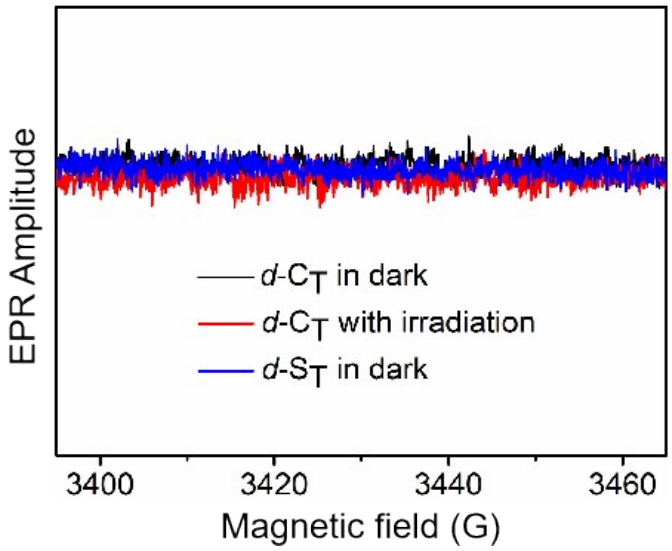

Figure S9 Electron spin resonance spectra of DMPO/***d*-S$_T$** in dark (blue) and DMPO/***d*-C$_T$** in 10 % DMSO-H_2O in dark (black) or light for 1 min (red).

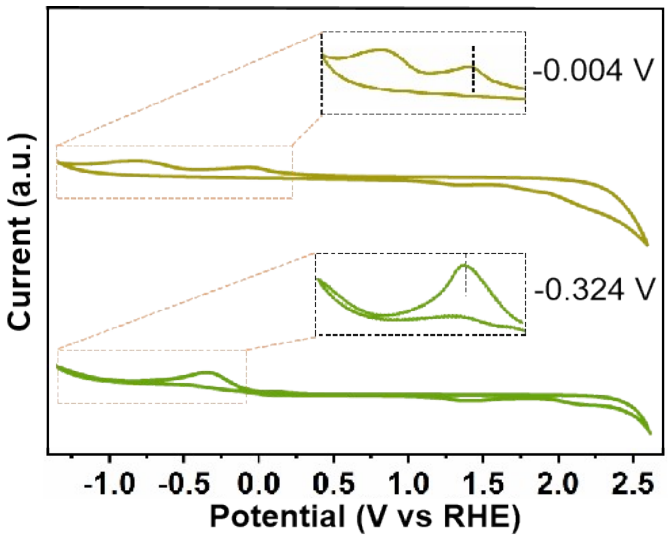

Figure S10 Cyclic voltammograms of ***d*-S$_T$** (green line) and ***d*-C$_T$** (yellow line) containing 0.1 M Tetrabutylammonium perchlorate. Scan rate: 100 mV/s

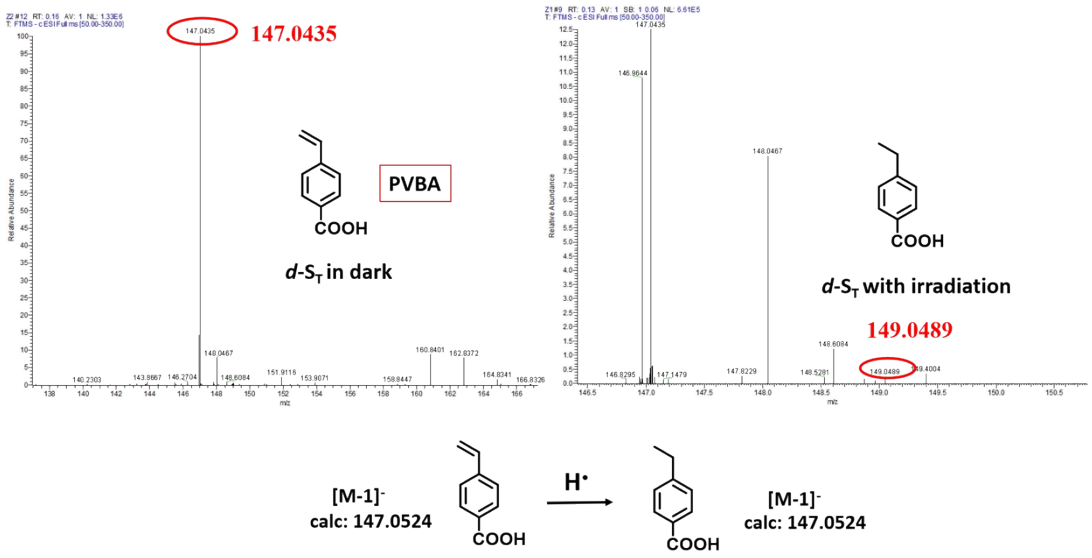

Figure S11 HRMS analysis of ***d*-S$_T$** containing PVBA (10 mM) under NIR light irradiation for 1 min.

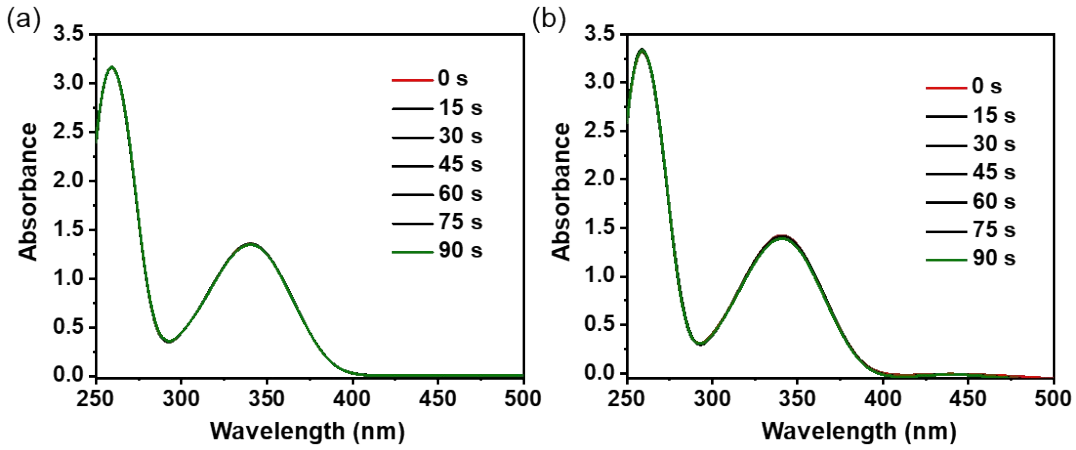

Figure S12 Photocatalytic oxidation for 90 s in air condition recorded by absorption spectra. (a) NADPH alone (50 μM); (b) ***d*-$\mathbf{C_T}$** (10 μM) + NADPH (50 μM).

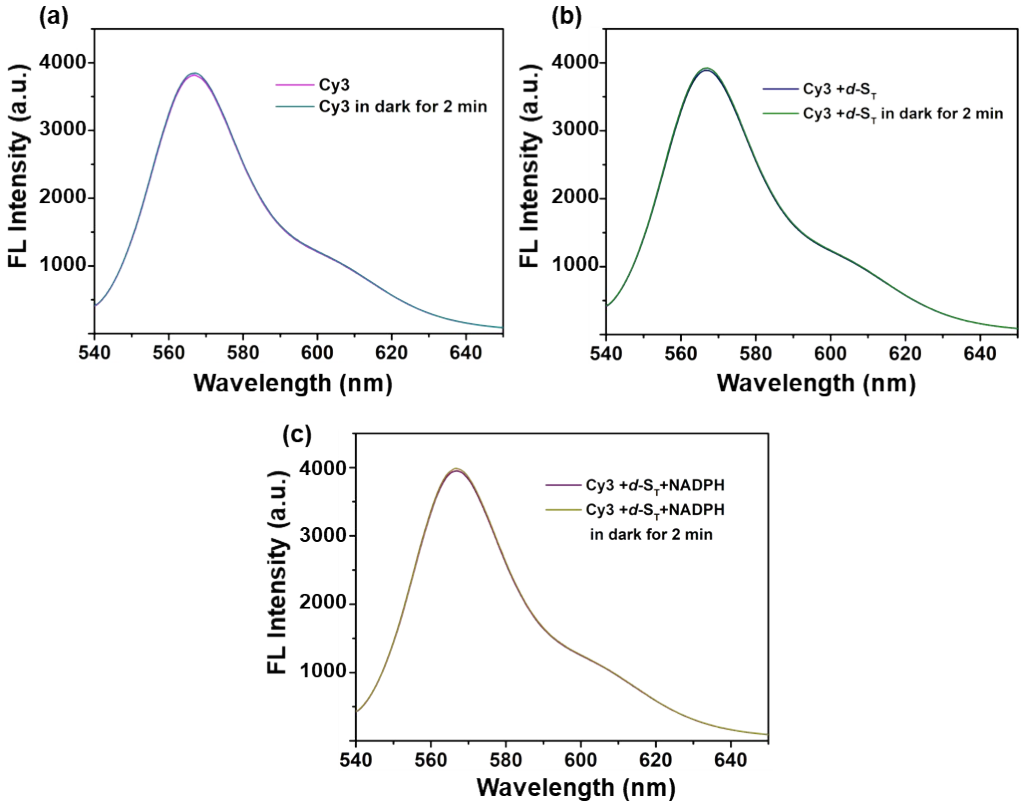

Figure S13 Detection of H• production in different treatment groups (Cy3, Cy3+ ***d*-$\mathbf{S_T}$**, Cy3+ ***d*-$\mathbf{S_T}$** + NADPH (50 μM)) in dark or in dark for 2 min in virtue of commercial fluorescent dye Cy3.

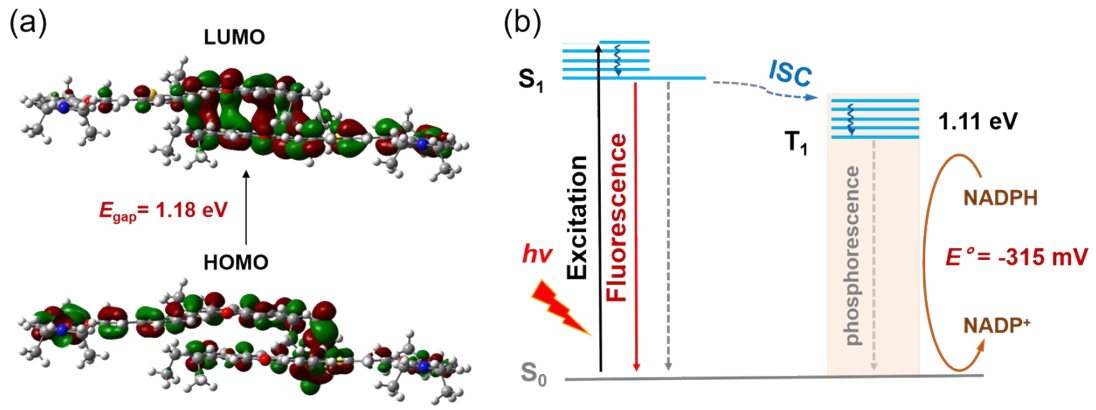

Figure S14 Frontier molecular orbital distributions and energy levels of ***d*-S$_T$** calculated using density functional theory (DFT) method at the B3LYP/6-31G (d, p) level.

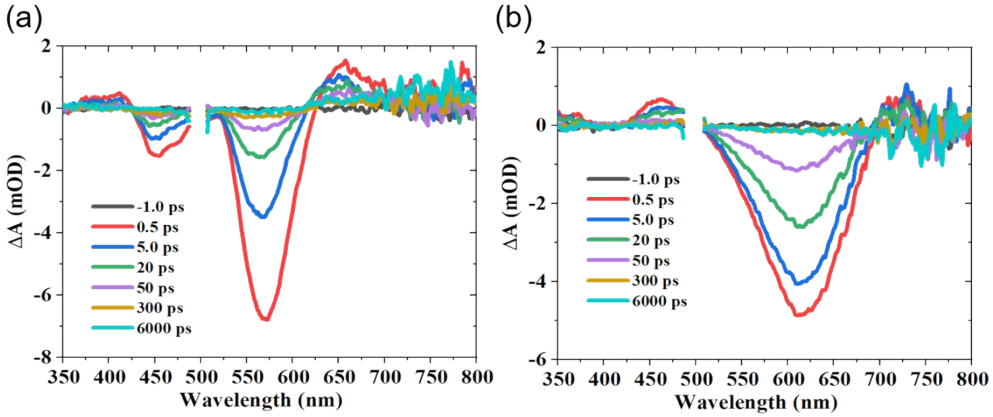

Figure S15 The analysis of transient absorption spectra of ***d*-S$_T$** and ***d*-C$_T$** in monomeric mode.

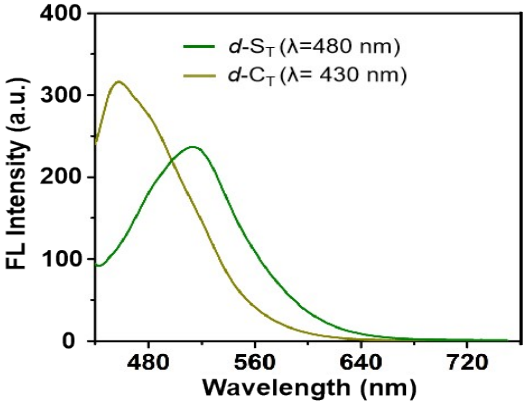

Figure S16 Fluorescence spectra of ***d*-S$_T$** (10 μM) and ***d*-C$_T$** (10 μM) aqueous solution.

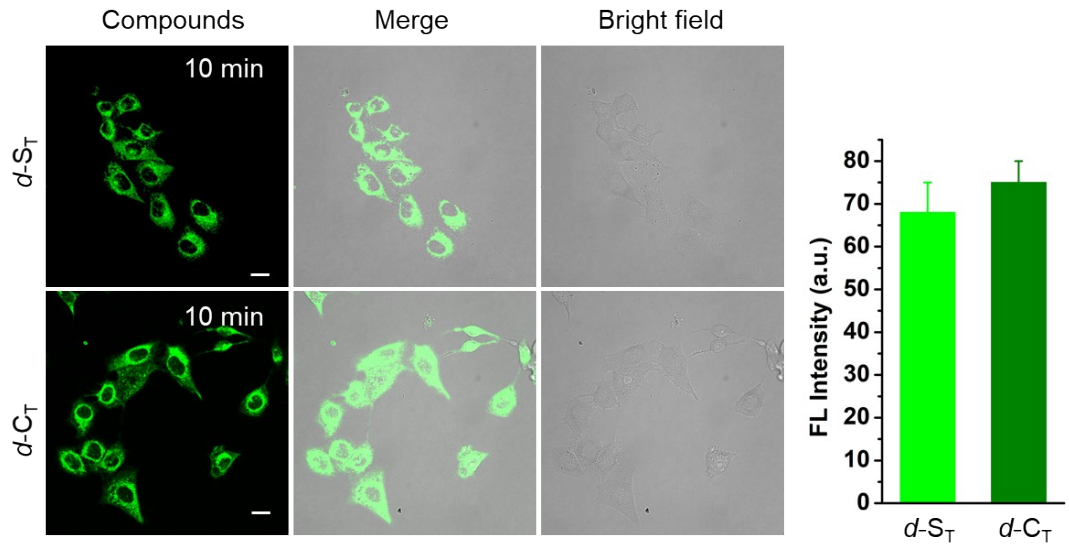

Figure S17 Cell imaging of HepG2 cells pretreated with *d*-S_T/*d*-C_T (10 μM) for 10 min. Scale bars: 20 μm.

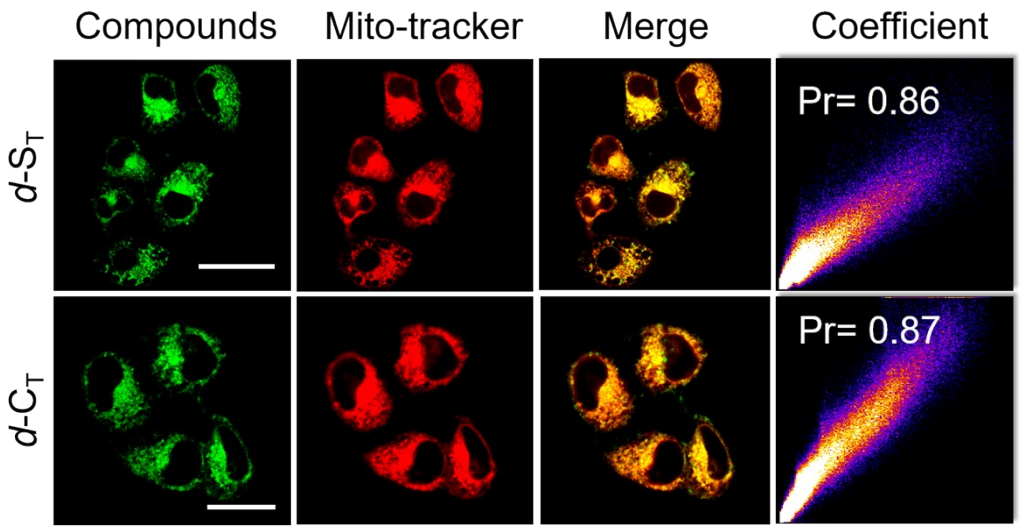

Figure S18 Colocalization images of the ***d*-S_T** (10 μM) and ***d*-C_T** (10 μM) for 30 min with Mito Tracker™ Deep Red FM (1 μM) in HepG2 cells. Scale bars: 20 μm.

Co-localization experiments demonstrated the red fluorescence arising from the commercial mitochondria probe (Mito TrackerTM Deep Red FM) merged well with the green fluorescence originating from ***d*-S_T/*d*-C_T** with a high Pearson correlation coefficient of 0.86 and 0.87, respectively, indicating their superior mitochondria targeting ability.

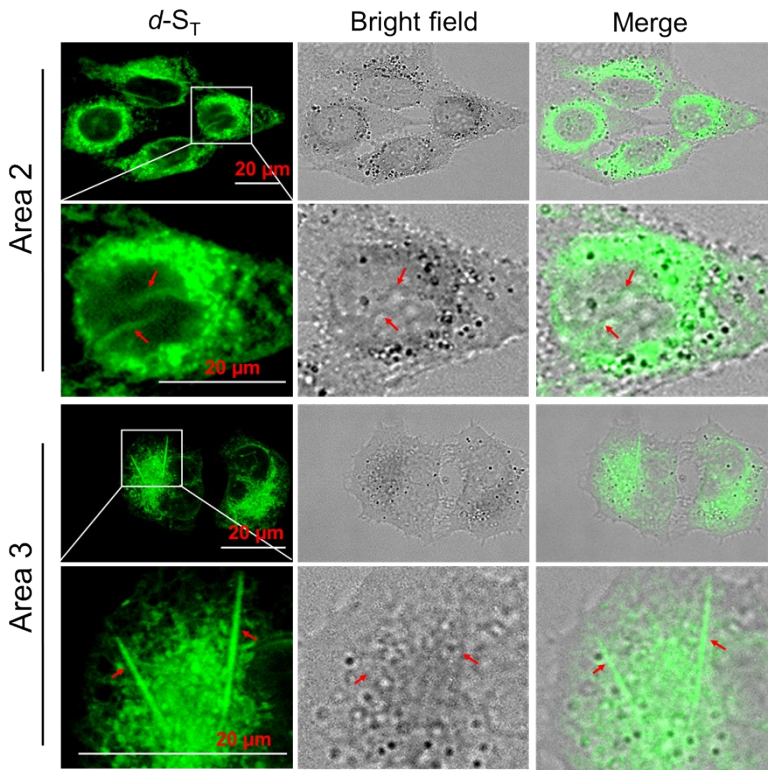

Figure S19 CLSM images of HepG2 cells following 30 min of incubation with ***d*-S$_T$** (10 μM) (self-assembly behavior in enlarged area: red arrow).

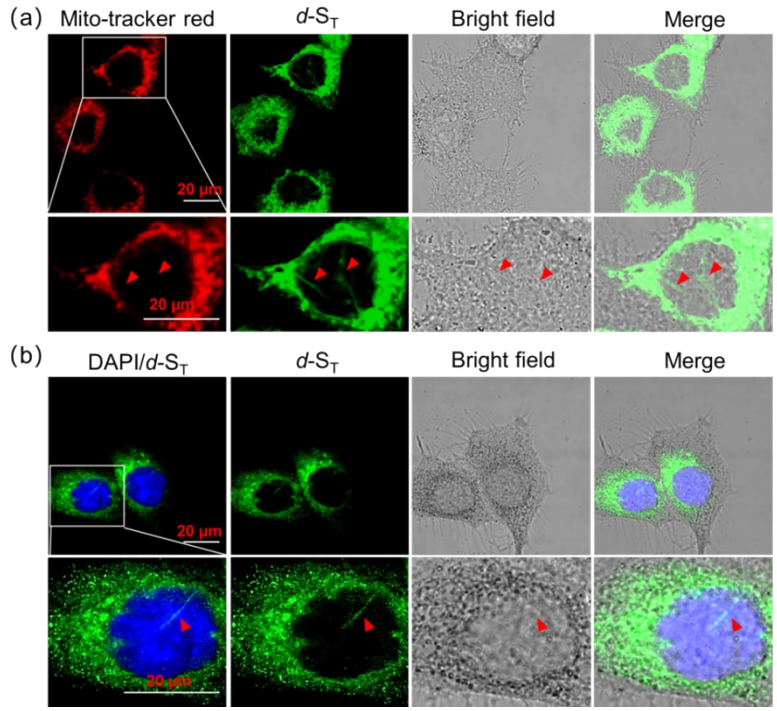

Figure S20 CLSM images of HepG2 cells following 30 min of incubation with ***d*-S$_T$** (10 μM) and 1 μM of commercial Mito-tracker red (a) and DAPI (b).

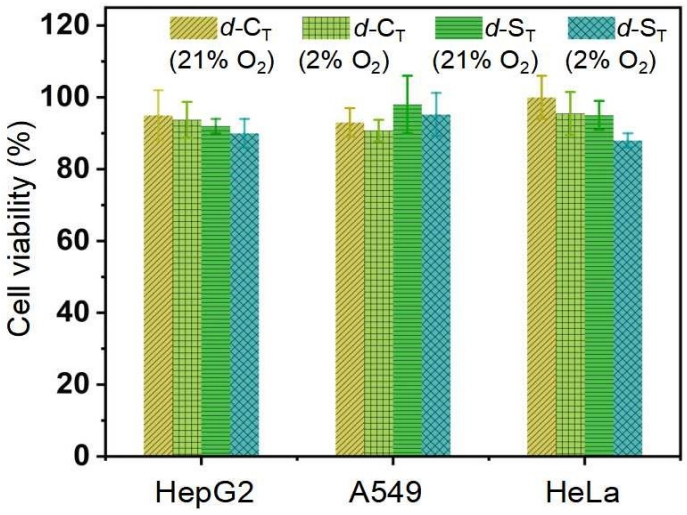

Figure S21 Cell viabilities in normoxia (21 % O_2) and hypoxia (2 % O_2) conditions of three cancer cells after treatment by ***d*-$\mathbf{C_T}$** (10 μM) or ***d*-$\mathbf{S_T}$** (10 μM) in dark condition.

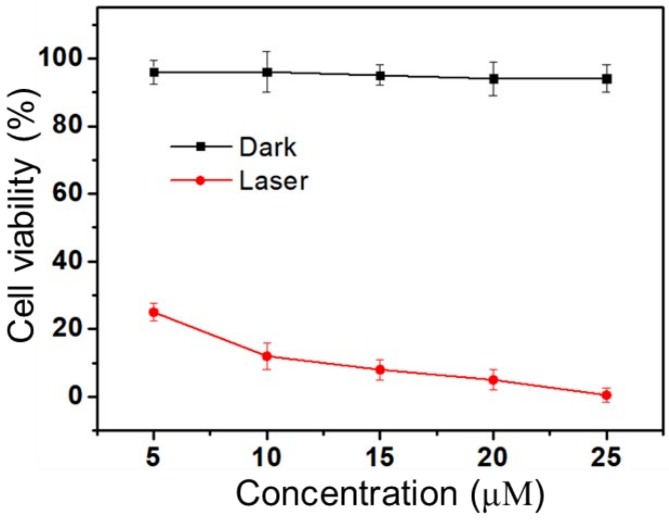

Figure S22 Cell viability of HepG2 cells incubated with various concentrations of *d*-S_T for 24 h with or without laser irradiation (660 nm; 0.2 W) for 2 min.

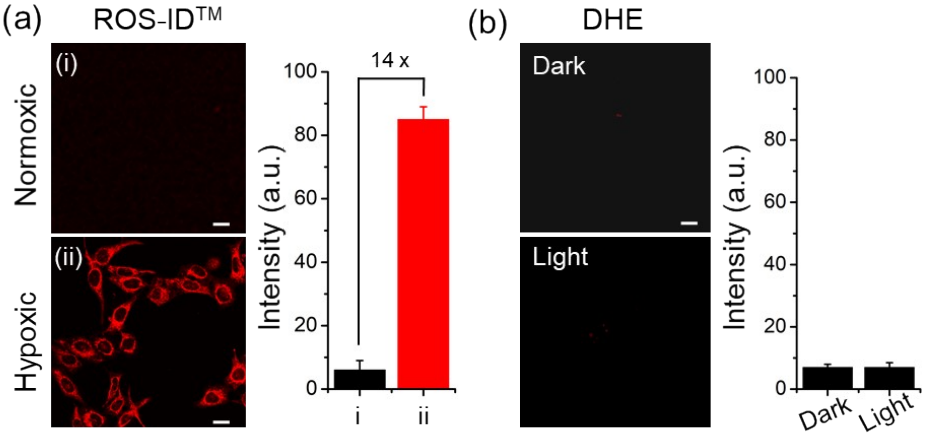

Figure S23 (a) Intracellular hypoxia imaging in virtue of ROS-ID as anaerobic indicator (b) Intracellular $O_2^{\bullet-}$ generation pretreated by ***d*-S$_T$** (10 μM) for 30 min with DHE as fluorescence probe by CLSM images. Scale bars: 20 μm.

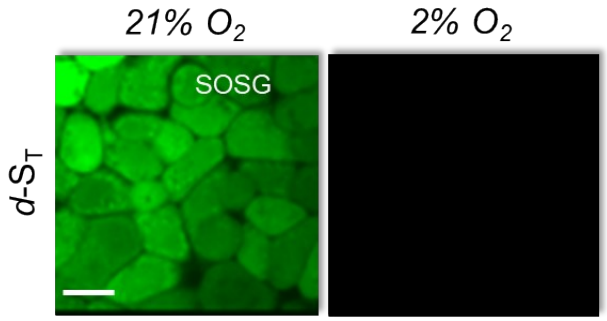

Figure S24 $^1O_2$ detection using commercial SOSG probe in HepG2 incubated with ***d*-S$_T$** (10 μM) and ***d*-C$_T$** (10 μM) cells for 30 min exposed to NIR light irradiation. Scale bars: 20 μm.

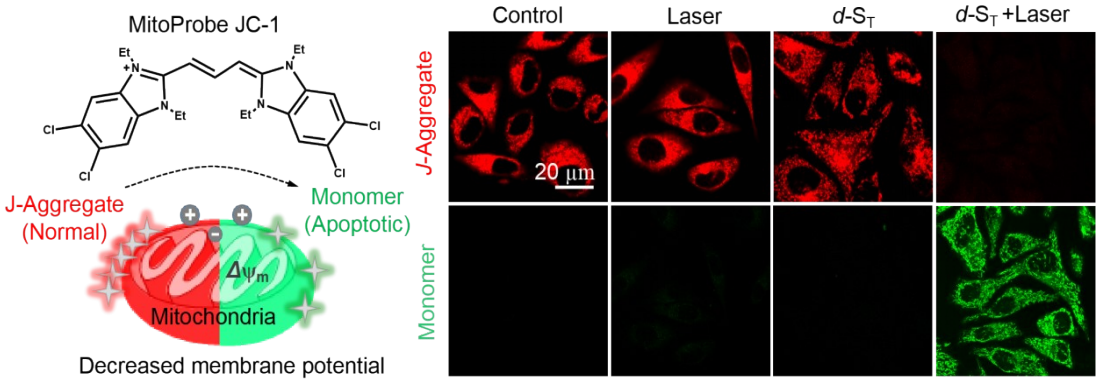

Figure S25 Detection of mitochondrial membrane potential in the HepG2 cells dealt with ***d*-S$_T$** (10 μM) for 30 min using JC-1.

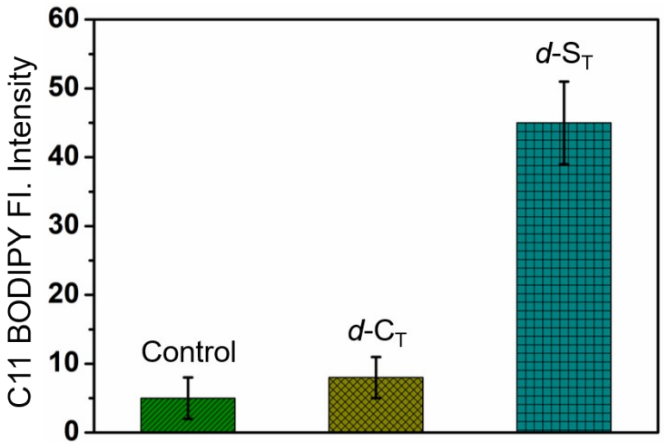

Figure S26 Fluorescence intensity change of C11-BODIPY stained cells for 30 min in different groups (Control; ***d*-C$_T$** and ***d*-S$_T$** (10 μM)).

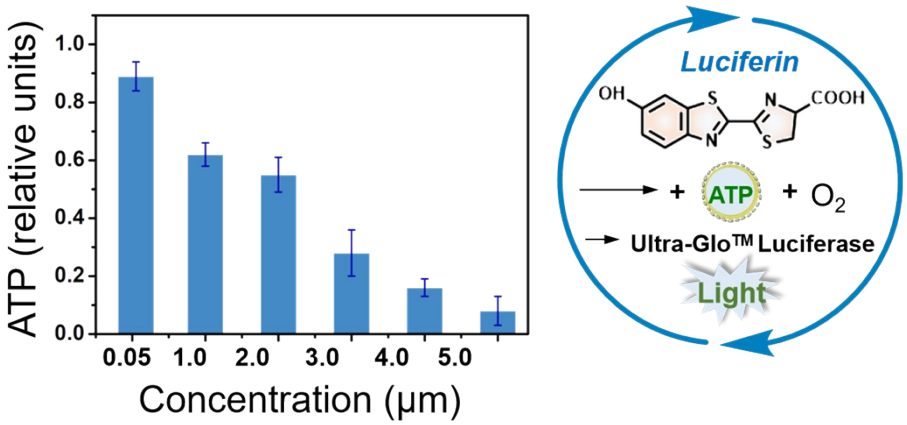

Figure S27 ATP detection in HepG2 cells treated with ***d*-S$_T$** (10 μM) by CLSM.

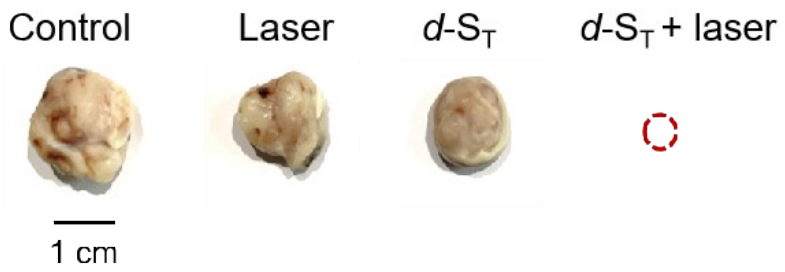

Figure S28 Images of tumors collected from mice of different groups after 18 days' treatments.

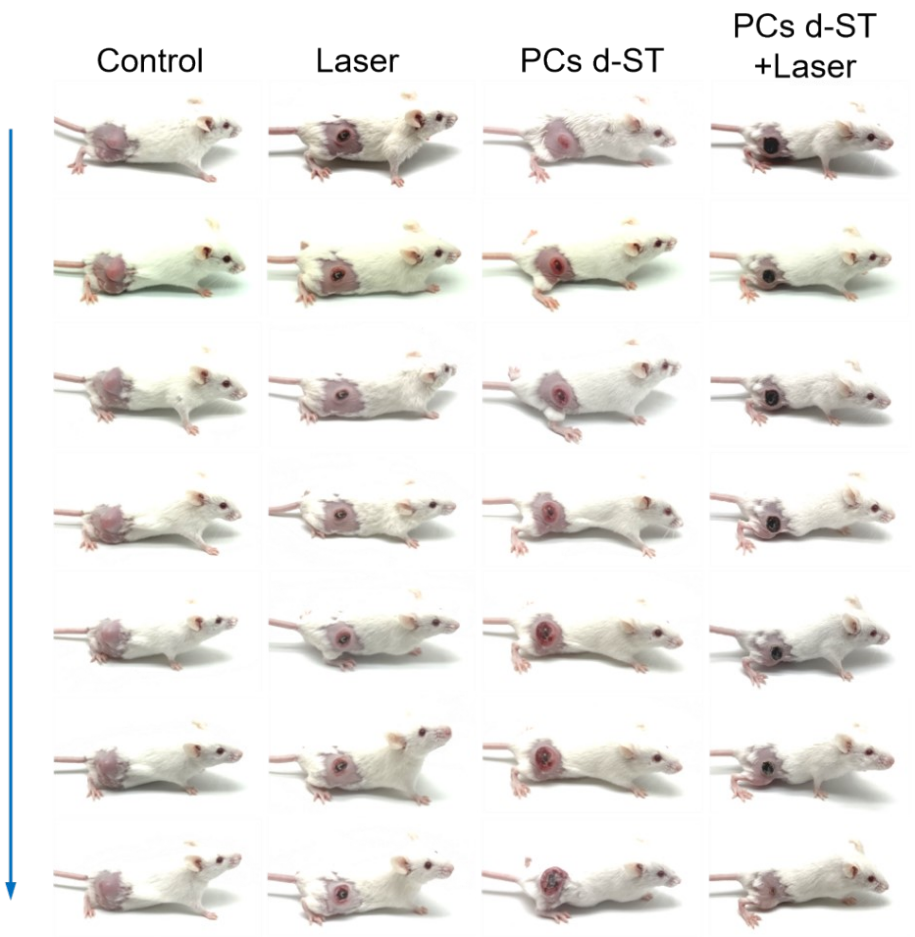

Figure S29 Photographs of four groups of mice after 18 days of photo therapy.

Reference

[S1]Bu, Y.; Zhu, X.; Wang, H.; Zhang, J.; Wang, L.; Yu, Z.; Tian, Y.; Zhou, H.; Xie, Y., *Analytical Chemistry* 2021, **93**, 12059-12066.

[S2]Huang, C.; Liang, C.; Sadhukhan, T.; Banerjee, S.; Fan, Z.; Li, T.; Zhu, Z.; Zhang, P.; Raghavachari, K.; Huang, H., *Angewandte Chemie International Edition* **2021**, 60, 9474-9479.

[S3]Guo, J.; Dai, J.; Peng, X.; Wang, Q.; Wang, S.; Lou, X.; Xia, F.; Zhao, Z.; Tang, B. Z., *ACS Nano* **2021**, 15, 20042-20055.

[S4]Wang, Y.; Mesdom, P.; Purkait, K.; Saubaméa, B.; Burckel, P.; Arnoux, P.; Frochot, C.; Cariou, K.; Rossel, T.; Gasser, G., *Chemical Science* **2023**, doi.org/10.1039/D3SC03932C

[S5]Li, M.; Xiong, T.; Du, J.; Tian, R.; Xiao, M.; Guo, L.; Long, S.; Fan, J.; Sun, W.;

Shao, K.; Song, X.; Foley, J. W.; Peng, X., *Journal of the American Chemical Society* **2019**, 141, 2695-2702